Experiments with Higdon's absorbing boundary conditions for a number of wave equations

W. A. Mulder

Shell International Exploration and Production B.V., Research and Technology Services, P.O. Box 60, 2280 AB Rijswijk, The Netherlands
E-mail: w.a.mulder@siep.shell.com

Received 13 December 1995; in final form 24 October 1996

Simulation of wave propagation for seismic purposes is usually restricted to a small portion of the earth. Artificial boundary conditions are required where the subsurface model is truncated. Absorbing boundaries should ensure that waves hitting the artificial boundaries are not reflected. The vast amount of literature on the subject suggests that "good" conditions have not been found, and only "reasonable" solutions exist. A cursory overview of existing and a few new ideas is presented that may guide the construction of suitable boundary conditions. Because the intended application of the boundary conditions was a high-order finite-difference code that runs on a parallel computer, we have restricted our attention to local boundary conditions. A fundamental problem in the design of accurate local boundary conditions is pointed out: accuracy is required to keep the amount of reflected energy small, but at the same time allows for growing low-frequency modes. We have settled for Higdon's boundary conditions. Higdon proposes to include some damping to suppress the growing low-frequency modes. We show that third-order conditions provide acceptable results for the simple scalar wave equation and the acoustic equation. In the elastic case, an additional low-frequency growing mode may occur. This mode can be suppressed by using a dissipative boundary scheme and by increasing the amount of damping. The increase in damping results in an increase in the amount of reflected energy, which is larger than in the scalar case. Numerical experiments exhibit a reasonable performance, although some improvement would be useful, particularly in the anisotropic elastic case.

Keywords: wave equation, finite differences, absorbing boundary conditions, anisotropy.

AMS subject classification: 65M06, 73B40, 86A15.

1. Introduction

Studies of wave propagation through the earth are often restricted to a small portion of the Earth's surface. Integration of the wave equation in such a setting requires artificial boundaries at the points where the model has been truncated. The simplest

and most reliable solution to this problem is the use of Dirichlet or Neumann boundary conditions and to choose a sufficiently large computational domain so that waves reflected from these boundaries do not have time to reach the receivers or the region under study. This may be a viable option for some two-dimensional computations. Often, computer time and storage are bottlenecks and the use of absorbing boundary conditions cannot be avoided. These conditions should ensure that waves hitting the artificial boundary are not reflected.

The vast amount of literature on the subject suggests that "good" absorbing boundary conditions have not been found, except in special cases or involving high computational cost, and only "reasonable" solutions exist. An extensive review can be found in [9].

Two aspects are important for absorbing boundary conditions: stability and accuracy. Stability ensures that the boundary conditions do not exhibit growing modes or spontaneously generated waves that propagate into the computational domain. Accuracy is needed to keep the amount of unwanted reflected energy small.

The stability theory for hyperbolic initial-boundary value problems is well developed. References are given in section 2. Although the stability theory can be used to check given conditions, it does not provide a means to construct optimal boundary schemes. Various ideas that may guide the construction of absorbing boundary conditions are reviewed in section 2 and some new ideas are added.

A fundamental problem is pointed out in section 2: accuracy and stability are contradictory requirements. This can be understood as follows. Consider a second-order formulation of the wave equation: $u_{tt} = c^2(u_{xx} + u_{yy} + u_{zz})$. For a constant velocity c, there exist solutions of the form t, xt, yt, and zt (t is time; x, y, and z are spatial coordinates). A discretisation of the wave equation of second or higher order will have these solutions as well. A sufficiently accurate absorbing boundary condition will also have these unwanted solutions. We thus have conflicting requirements: the boundary conditions should be sufficiently accurate to avoid strong reflections, whereas the modes mentioned above should be suppressed. This problem appears to have been overlooked by many authors except a few [14].

In section 3, we consider Higdon's boundary conditions [16–18]. These conditions are attractive because they are local and therefore relatively easy to use in a parallel finite difference code, and they can be used not only for the scalar wave equation but also for the elastic case. Higdon's conditions require some damping to suppress low-frequency waves that are allowed to grow by the weakly ill-posed nature of the boundary conditions. We apply the scheme for a sequence of points near the boundary rather than just for one point on the boundary. In this way, the boundary conditions can be easily combined with the high-order difference schemes used for the wave equation. The scheme has been tested for the simple wave equation, the acoustic wave equation, and the isotropic and anisotropic elastic wave equation. In the elastic case, the corners of the computational domain need special attention.

Section 4 presents some numerical experiments and examples.

2. Overview

Stability and accuracy of absorbing boundary conditions are the two main issues. Here we will give a cursory review of results.

The *stability* theory for initial-boundary value problems has been established in a paper by Gustafsson et al. [11] (see also [15]). Their stability criterion is commonly referred to as *GKS* stability. Two approaches are considered: the energy method and normal mode analysis. The first is based on determining bounds on a suitable energy norm and is generally restricted to problems with homogeneous boundary data. The second is based on local mode analysis, using the z-transform (the discrete Laplace transform). The boundary scheme and the interior difference scheme have to be analysed simultaneously. By using the z-transform in time and space, a linear system of equations is obtained. A necessary condition for stability is that there be no eigensolutions that represent growing modes propagating into the interior domain. This condition, however, is not sufficient: small perturbations of the data may cause a marginally stable scheme to become unstable anyway. To account for such instabilities, the notion of so-called generalised eigenvalues is introduced. These generalised eigenvalues should not occur in a boundary scheme. An interpretation of the stability criteria in the case of normal mode analysis has been given in [32, 33] in terms of reflection coefficients and group velocities. The occurrence of growing incoming modes can be interpreted as a reflection coefficient being larger than one in size. The occurrence of generalised eigenvalues corresponds to modes that have a group velocity of the wrong sign so that they move into the domain.

Goldberg and Tadmor have derived "convenient stability criteria" [10]. They introduced *translatory* and *solvable* boundary conditions: the same formula is used for a sequence of points at the boundary, and the boundary scheme and the interior difference scheme should both be stable. They prove that if at least one of these schemes is *dissipative*, then the combination of the interior and boundary scheme is stable as well. These translatory boundary conditions are attractive for higher-order difference schemes, because the stability analysis can be carried out independently of the interior scheme and only one expression needs to be analysed and implemented. However, their result is only proven for one-dimensional problems.

Michelson [26] has extended parts of the GKS stability theory to multi-dimensional problems, but with the restriction that the hyperbolic system be *dissipative*. Corners in multi-dimensional problems are a known source of trouble [2, 27].

The *accuracy* of the boundary conditions is another issue. Gustafsson [12, 13] has shown that the local order of accuracy of the boundary scheme may be lower than that of the interior scheme, without affecting the global accuracy of the numerical solution. This can be understood by realising that some of the errors generated by the boundary scheme leave the computational domain.

The GKS stability theory allows to assess whether or not a given boundary scheme can be used. This still leaves the question which boundary scheme to choose. Various types of boundary conditions have been proposed in the literature, based on different ideas. These ideas can be roughly divided into four classes:

1. schemes based on an approximation of the one-way wave equation;
2. schemes based on some damping mechanisms;
3. schemes based on extrapolation of data from the interior;
4. other.

We will illustrate the basic ideas for the one-dimensional equation $u_{tt} = c^2 u_{xx}$ or the two-dimensional equation $u_{tt} = c^2(u_{xx} + u_{yy})$. The propagation speed c is assumed to be constant. In the examples, we will consider the "left" boundary at constant x.

2.1. One-way wave equation

Boundary conditions for one-dimensional problems can be obtained in a direct manner by using a characteristic decomposition. The wave equation with constant c can be factored as

$$\left(\frac{\partial^2}{\partial t^2} - c^2\frac{\partial^2}{\partial x^2}\right)u = \left(\frac{\partial}{\partial t} + c\frac{\partial}{\partial x}\right)\left(\frac{\partial}{\partial t} - c\frac{\partial}{\partial x}\right)u.$$

For a boundary at the left-hand side of the computational domain, we only want left-going waves, so near the boundary the original equation is replaced by

$$\left(\frac{\partial}{\partial t} - c\frac{\partial}{\partial x}\right)u = 0. \tag{1}$$

The discrete version should honour the left-going character by using an appropriate one-sided discretisation. For multi-dimensional problems, this factorisation can only be carried out approximately. The simplest approximation is the one-dimensional expression (1). Out of many references we mention [1, 31]. This works fine for plane waves that propagate in a direction perpendicular to the boundary, with zero angle of incidence, but not for waves impinging at larger angles.

Additional terms can be added to (1) to reduce the reflection of waves at larger angles of incidence [5, 7, 8, 34]. The derivation proceeds as follows. Consider the Fourier transform of u:

$$\widehat{u} = \exp\left[\mathrm{i}(k_1 x + k_2 y + \omega t)\right].$$

A left-going wave must obey

$$k_1 = \frac{\omega}{c}\sqrt{1 - \left(\frac{ck_2}{\omega}\right)^2}, \tag{2}$$

and the corresponding boundary condition is

$$\left[\partial_x - \mathrm{i}\frac{\omega}{c}\sqrt{1 - \left(\frac{ck_2}{\omega}\right)^2}\right]\widehat{u} = 0.$$

In principle, this can be implemented by using Fourier transforms, assuming that c is constant on the boundary. Because this is often impractical and restrictive, *local* approximations can be obtained by finding a suitable expansion of the square-root in (2). For $(ck_2/\omega)^2 \ll 1$, the lowest order Taylor series expansion leads to

$$\left[\partial_x - \frac{1}{c}\partial_t\right] u = 0,$$

whereas the next order provides an operator

$$\partial_x - \mathrm{i}\frac{\omega}{c} + \frac{1}{2}\mathrm{i}\frac{ck_2^2}{\omega},$$

which, after multiplication by $\mathrm{i}\omega$ and transformation back to u, leads to

$$u_{tt} = cu_{xt} + \frac{1}{2}c^2 u_{yy}. \tag{3}$$

If the next term in the Taylor series expansion is taken into account, the resulting boundary condition turns out to be *strongly* ill-posed [7], meaning that the boundary condition allows for a nontrivial solution that propagates into the domain (this may be interpreted as an "infinite reflection coefficient" [32]). However, if a rational (Padé) expansion is used instead, well-posed boundary conditions of higher order can be obtained [7, 8]. These approximations are given, recursively, by

$$\begin{aligned} \mathcal{B}_1 &= \partial_t - c\partial_x, \\ \mathcal{B}_2 &= 2\partial_t^2 - 2c\partial_x\partial_t - c^2\partial_y^2, \\ \mathcal{B}_{M+1} &= 2\partial_t\mathcal{B}_M - c^2\partial_y^2\mathcal{B}_{M-1} \quad (M > 1), \end{aligned} \tag{4}$$

leading to the condition $\mathcal{B}_M u = 0$ at the boundary. If the interior differential equation is used to eliminate the y-derivatives, the resulting boundary operator simplifies to

$$B_M = (\partial_t - c\partial_x)^M \quad (M > 0). \tag{5}$$

The corresponding reflection coefficient for a wave with angle of incidence θ is

$$R = \left(\frac{1-\cos\theta}{1+\cos\theta}\right)^M,$$

which shows that higher-order boundary conditions reduce the size of the reflection coefficient, but also that the wide-angle approximations still fail for waves at grazing incidence. Moreover, the resulting boundary conditions may still be *weakly* ill-posed [14] (contrary to what is claimed in [7, 8]). This is caused by "generalised eigenvalues": small perturbations of the boundary conditions result in waves that move into the

computational domain, causing polynomial growth of the solution. Gustafsson's cure for (3) is

$$u_t = cu_x + \frac{1}{2}c^2 \int_0^t u_{yy}\,\mathrm{d}t. \tag{6}$$

To illustrate what the problem is and why Gustafsson's cure works, a simple example based on polynomials rather than the usual Fourier and Laplace transforms suffices. The wave equation cannot "see" functions of the form

$$n(t,x,y) = a_0 + a_{1,0,0}t + a_{0,1,0}x + a_{0,0,1}y + a_{1,1,0}tx + a_{1,0,1}ty + a_{0,1,1}xy. \tag{7}$$

The boundary condition $\mathcal{B}_1$ at $x = 0$ reduces this to

$$n_1(t,x,y) = (a_0 + a_{0,0,1}y) + (a_{0,1,0} + a_{0,1,1}y)(x + ct). \tag{8}$$

The boundary condition $\mathcal{B}_2$, on the other hand, only imposes $a_{1,1,0} = 0$, implying that there may be growing solutions of the form t and yt. Gustafsson's cure provides the same result as in (8) for the assumed form of the solution (7).

The authors of [7, 8] prove well-posedness of the boundary conditions $\mathcal{B}_n$, but use conditions from [21] that are valid for *first-order* systems. The second-order formulation adds the complication of a larger null-space, i.e., solutions of the form xt and so on. This has apparently been overlooked by many authors, but amended by Gustafsson [14] by returning to a first-order formulation of the boundary condition.

Another approach to the problem of waves at large angles of incidence is given by Lindman [24]. Its generalisation to the elastic case can be found in [28]. The idea is to write the boundary condition as

$$u_t - \frac{c}{\cos\theta}u_x = 0, \tag{9}$$

where θ is the angle of incidence of an incoming wave. A rational approximation for $1/\cos\theta$ is made, with coefficients that depend on the solution. The coefficients obey wave-like partial differential equations in a region near the boundary, which have to be solved separately. The coefficients are then used to act as a source term in the boundary condition that represents that rational approximation to (9). Results in [24] and [28] suggest that these boundary conditions are weakly ill-posed, although the authors only mention problems with "evanescent" waves.

The apparent normal velocity can also be estimated directly from the solution, resulting in a *nonlinear* boundary scheme. An example is

$$\cos\theta = \sqrt{1 - \left(\frac{cu_y}{u_t}\right)^2},$$

with the right-hand side set to 0 if $u_t = 0$ or for imaginary results. Another example can be found in [3]. These boundary conditions are not very effective in combination with higher-order interior schemes, as we have observed in numerical experiments.

2.2. Damping

Boundary conditions based on some damping mechanism are usually easy to implement and can be made to work well for waves at grazing incidence. They are generally less effective for waves at normal incidence. A simple scheme [4, 22] is obtained by multiplication of the displacement field and its time-derivative by a smooth taper: a function that is one in the interior and slightly less than one in a boundary strip. This approach can be viewed as an approximation to

$$u_{tt} = c^2(u_{xx} + u_{yy}) - 2(1-\gamma)u_t - (1-\gamma)^2 u,$$

where γ is the taper. The width of the boundary strip needs to be rather large if strong low-frequency reflections are to be avoided. Our own experiments with a strip of 16 boundary points and a smoothly decreasing taper show that this boundary condition performs less well if the grid is refined. A remedy is to increase the width of the strip at the same time, implying that the percentage of points used for the boundary conditions remains fixed under grid refinement and may be relatively large. This is not very attractive for three-dimensional computations, where computer memory is often a bottleneck.

A similar idea can be found in [30], where an equation of the form

$$u_{tt} + (1-\gamma)u_t = c^2(u_{xx} + u_{yy})$$

is considered.

"Sponge" boundaries [6, 20] may improve the boundary scheme for waves at normal incidence: the damping equation in the boundary strip is taken to be

$$u_{tt} + (1-\gamma)(u_t - cu_x) = c^2(u_{xx} + u_{yy}),$$

thus emphasising the damping of the reflected waves.

Boundary schemes based on damping are robust, easy to code, and do not suffer from the weakly ill-posed behaviour mentioned above. On the other hand, they require careful tuning of the number of points in the boundary strip and the shape of the taper function that determines the damping.

2.3. Extrapolation

Finite difference schemes for the wave equation usually need data outside the computational domain if the same difference scheme is used everywhere. These additional data can be provided by numerical extrapolation of the interior data. The simplest form of extrapolation is one-dimensional in the direction perpendicular to the artificial boundary. This may be generalised by using data from earlier time steps and from the coordinate directions parallel to the boundary. Here we will only consider one-dimensional space and space–time extrapolation.

Let the grid spacings be denoted by Δx and Δy, the time step by Δt. Time is $t^n = n\Delta t$. The y-direction is ignored, because we will only consider one-dimensional

extrapolation. The discrete solution at (t^n, x_j) is denoted by u_j^n. The left boundary is positioned at $j = 0$.

A simple spatial extrapolation scheme can be obtained by using an interpolating polynomial through M points from the interior domain. The resulting expression for the boundary values is

$$u_j^n = \sum_{i=1}^{M} \binom{M}{i} (-1)^{i+1} u_{j+i}^n, \quad j = 0, -1, \ldots . \tag{10}$$

Here as many values of $j \leqslant 0$ can be computed as needed, marching away from the boundary. Space–time extrapolation along the line $x + t = 0$ is given by

$$u_j^n = \sum_{i=1}^{M} \binom{M}{i} (-1)^{i+1} u_{j+i}^{n-i}, \quad j = 0, -1, \ldots . \tag{11}$$

Boundary conditions of these types are used as examples in [10].

Equation (10) may be viewed as a discretisation of $\partial_x^M u = 0$ at the boundary and equation (11) as a discretisation of

$$\left(\partial_t - \frac{\Delta x}{\Delta t} \partial_x \right)^M u = 0.$$

Therefore, it will come as no surprise that these boundary conditions are weakly ill-posed for $M > 1$ if used in combination with the second-order wave equation.

Obvious generalisations are

$$(\partial_t - c\partial_x)^M u = 0, \tag{12}$$

as described in [23] and analysed in [16]. A further generalisation is

$$\prod_{i=1}^{M} \left(\frac{\partial}{\partial t} - c_i \frac{\partial}{\partial x} \right) u = 0, \tag{13}$$

as analysed by Higdon in [17, 18]. Here the velocities c_i can be chosen so as to minimise the reflection coefficient. A plane wave at an angle of incidence θ to the normal will have an apparent velocity $c/\cos\theta$. By setting $c_i = c/\cos\theta_i$ and choosing θ_i, the reflection coefficient for any wave can be kept small. This approach can also be used for the elastic case by treating components of the displacement separately.

Note that equations (12) and (13) have originally been applied by the authors only one point deep ($j = 0$). Therefore, they may be better classified as approximations to the one-way wave equation similar to (5). Again, these boundary conditions are weakly ill-posed for $M > 1$ if used in combination with the second-order wave equation.

2.4. Other tricks

Here we mention a few other approaches. An obvious one is grid stretching: if the grid spacing is gradually increased in the direction of the outward normal, a wave that hits the boundary will take a long time to cross this region (stretching the grid has the same effect as lowering the velocity in the normal direction while keeping the normal component of the impedance constant). This approach has two disadvantages:

(i) The stretching should be gradual enough to avoid unwanted reflections. This implies that the computational domain must be extended by a rather large number of points.

(ii) A larger grid spacing generates larger numerical errors. Waves become more high-frequent with respect to the grid, and errors are larger for higher frequencies. The highest frequencies that can be represented on a grid have no propagation direction (e.g., a wave of the form $\{+1, -1, +1, -1, \ldots\}$ on subsequent grid points in one space dimension). Once some frequencies are transformed into the highest frequency, they generate waves that actually turn back towards the interior and lower their apparent frequency in the process. This leads to substantial reflection. Obviously, the effect can be reduced by adding more points ...

An *exact* approach can be found in [29]: instead of absorbing conditions, full reflection is used. A Dirichlet boundary condition ($u = 0$) produces a reflected wave with opposite sign, a Neumann boundary condition ($u_x = 0$) produces a reflection with the same sign as the original wave. Adding these two together provides a perfect absorbing boundary. The price paid is that the number of required computations doubles as soon as a wave reflects against the boundary. If a strong reflector sits close to a boundary, a wave will bounce rapidly back and forth between the boundary and reflector. This will cause a rapid and prohibitive increase of cost. Therefore, this method is useless for geophysical applications.

Nevertheless, we were tempted to carry this idea further. Is there a way to avoid the blow-up in cost? The following idea was tried. Suppose we have a region Ω_b near the boundary where an incoming signal $u(t, x, y)$ is split as follows:

$$u = u^+ + u^-, \quad u^+ = \max(0, u), \; u^- = \min(0, u).$$

Inside Ω_b, we integrate two wave equations, one for u^+ and one for u^- with Dirichlet boundary conditions. After each time step, we reset $u^+ = \max(0, u^+)$ and $u^- = \min(0, u^-)$. The splitting of u is carried out in the interior domain in a region adjacent to Ω_b and the resulting u^+ and u^- are used as boundary data. At the opposite end, a Dirichlet boundary is used with $u = 0$. Both u^+ and u^- are reflected with opposite sign and the reflected waves are removed by the "reset" operation performed after each time step.

This method works perfectly well as long as incoming waves have a distance between zero-crossings of u in the direction perpendicular to the boundary that fits inside the domain Ω_b. This disqualifies the method for waves at grazing incidence that may have extremely large apparent wavelengths.

We end this section by remarking that endless combinations of the above methods can be made, and are being made by numerous authors.

3. Higdon's boundary scheme

We needed good absorbing boundary conditions for a parallel high-order finite-difference code that integrates several types of wave equations in one, two, and three space dimensions. The equations are: the simple wave equation (constant density acoustics), the acoustic wave equation, and the isotropic and anisotropic elastic system of equations. Before proceeding with the motivation for the choice of Higdon's conditions, we mention our choice of interior discretisation schemes.

The simple wave equation reads

$$u_{tt} = f + c^2 \Delta u. \tag{14}$$

Here $f = f(t, x, y, z)$ denotes a source term. This equation is discretised by a high-order *central* difference scheme that approximates the second derivatives directly. The acoustic wave equation reads

$$\frac{1}{\rho c^2} u_{tt} = f + \nabla \cdot \frac{1}{\rho} \nabla u, \tag{15}$$

and is discretised by *staggered* finite differences. The system of elastic equations is

$$\rho u^{(k)}_{tt} = f^{(k)} + \sum_{\ell=1}^{3} \partial_\ell \sigma^{(k,\ell)}, \quad k = 1, 2, 3. \tag{16}$$

Here $\partial_1 = \partial_x$, $\partial_2 = \partial_y$, and $\partial_3 = \partial_z$. The displacement in the x-direction is $u^{(1)}$, in the y-direction $u^{(2)}$, and in the z-direction $u^{(3)}$. The stress $\sigma^{(k,\ell)}$ is related to the strain $\varepsilon^{(m,n)}$ by

$$\sigma^{(k,\ell)} = \sum_{m=1}^{3} \sum_{n=1}^{3} C^{(k,\ell,m,n)} \varepsilon^{(m,n)}, \quad \varepsilon^{(m,n)} = \frac{1}{2} \big(\partial_m u^{(n)} + \partial_n u^{(m)} \big). \tag{17}$$

Here $C^{(k,\ell,m,n)}$ is the elasticity tensor. These equations are discretised by staggered finite differences. Details can be found in appendix B.

The following considerations guided the choice of a boundary scheme. The spatial order of the difference scheme is usually chosen to be $N_x = 8$, and the temporal order $N_t = 2$ or $N_t = 4$. The simplest option, damping as in [4, 22], did not work satisfactorily. Some improvement could be made by additional grid stretching, but the overall performance was too sensitive to the actual number of extra points in the boundary strip and the parameters of the damping function.

Extrapolation schemes appeared to be the next attractive option. Per time step, the finite difference scheme needs N_e additional points, where $N_e = N_t N_x/4$ for the simple wave equation (14), $N_e = N_t(N_x - 1)$ for the anisotropic elastic case, and $N_e = N_t(N_x - 1)/2$ otherwise. Therefore, a translatory scheme appeared attractive, to provide the additional N_e data points per point on the boundary. The spatial and

temporal order of this scheme can be allowed to be lower than those of the interior scheme [12, 13]. We are not so much interested in the formal order of the boundary scheme as in keeping the reflections small. Reflection coefficients of at most a few percent are acceptable, given the numerical errors incurred in the interior.

Note that the values of N_e listed above apply to an extrapolation applied to the primary variables $u^{(k)}$ only. For the elastic equation, the extrapolation might be carried out for both the displacement field and the normal stress components, thus decreasing the width of the boundary strip but doubling the number of components. This approach can be used even in the second-order formulation of the elastic wave equation. The computed stresses are discarded after the acceleration has been computed, so the normal components required for extrapolation have to be stored separately. This only involves a relatively small amount of data. This approach has not been pursued because of its increased complexity in a parallel computing environment.

The schemes $\mathcal{B}_1$ and $\mathcal{B}_2$ proved unsatisfactory, as did the modified version (6), the reason being mainly that the reflection coefficient was not small enough for waves at large angles of incidence. We also considered a third-order version of Higdon's boundary condition (13). These conditions need a fix against blow-up caused by their weakly ill-posed nature. Higdon [17, 18] proposes the inclusion of an $\mathrm{O}(\Delta t)$ damping term:

$$\left[\prod_{i=1}^{M}\left(\frac{\partial}{\partial t}-c_i\frac{\partial}{\partial x}+\varepsilon^*_{i-1}\right)\right]u=0. \tag{18}$$

An equivalent formulation in the case of zero ε^*_0 is

$$Q_1 u = 0, \tag{19}$$

where

$$\begin{aligned} Q_i &= \left(\frac{\partial}{\partial t}-c_i\frac{\partial}{\partial x}\right)\big(\widetilde{\varepsilon}_i+(1-\widetilde{\varepsilon}_i)Q_{i+1}\big), \quad 1\leqslant i\leqslant M-1,\\ Q_M &= \left(\frac{\partial}{\partial t}-c_M\frac{\partial}{\partial x}\right), \end{aligned} \tag{20}$$

and the $\widetilde{\varepsilon}_i\Delta t$ are small positive constants. These constants are introduced to suppress the above mentioned null-space problems, which tend to show up as slowly growing long-wave instabilities.

The boundary scheme is used in combination with interior difference schemes of high order. To do so requires the application of the same scheme to N_e points in the boundary strip, marching from the interior to the outer edge. For this boundary scheme, M points are needed from the interior.

We use the third-order scheme ($M=3$). For the wave equation, each of the first-order factors has been discretised by a one-sided implicit scheme that is second-order-accurate in space and time (24). In the third-order case, this leads to a boundary operator

$$R_1\big[\varepsilon_1+(1-\varepsilon_1)R_2\big\{\varepsilon_2+(1-\varepsilon_2)R_3\big\}\big], \tag{21}$$

with

$$R_j = 1 - z^{-1}T + \frac{1-\nu_j}{1+\nu_j}\big(T - z^{-1}\big).$$

Here $\nu_j = c_j\Delta t/\Delta x$ is the local *Courant–Friedrichs–Lewy* (CFL) number. The shift operator in space is denoted by T and in time by z, i.e., $T^m u_j^n = u_{j+m}^n$ and $z^m u_j^n = u_j^{n+m}$ for integer m. Here the discrete solution at time $t^n = n\Delta t$ and position $x_j = j\Delta x$ is denoted by u_j^n, as before. Numerical experiments with this scheme will be presented in the next section.

This scheme does not perform well for the elastic equations, because a growing low-frequency mode exists that does not occur for the scalar wave equations. This mode can be found as follows. Consider the isotropic homogeneous elastic P-SV case in two space dimensions x and z:

$$\begin{aligned}
\rho\partial_{tt}u^{(1)} &= (\lambda+\mu)\big(\partial_{xx}u^{(1)} + \partial_x\partial_z u^{(3)}\big) + \mu\big(\partial_{xx}u^{(1)} + \partial_{zz}u^{(1)}\big),\\
\rho\partial_{tt}u^{(3)} &= (\lambda+\mu)\big(\partial_x\partial_z u^{(1)} + \partial_{zz}u^{(3)}\big) + \mu\big(\partial_{xx}u^{(3)} + \partial_{zz}u^{(3)}\big),
\end{aligned}$$

defined on the quarter plane $x \geqslant 0$, $z \geqslant 0$, together with undamped second-order boundary conditions at $x = 0$ and $z = 0$. Here $\lambda = \rho(c_p^2 - c_s^2)$ and $\mu = \rho c_s^2$; ρ is the density and c_p and c_s are the pressure and shear velocities. The x- and z-displacements are denoted by $u^{(1)}$ and $u^{(3)}$, respectively. The boundary conditions read

$$(\partial_t - c_1\partial_x)(\partial_t - c_2\partial_x)u^{(i)}(x,0) = 0, \quad i = 1,3,$$

and

$$(\partial_t - c_1\partial_z)(\partial_t - c_2\partial_z)u^{(i)}(0,z) = 0, \quad i = 1,3.$$

Apart from a constant and functions linear in x, z, and t, the equations allow for a solution of the form

$$\begin{aligned}
u^{(1)} &= a_0t^2 + a_1x^2 + a_2z^2 + \frac{2t}{c_1+c_2}\big[(a_0 + a_1c_1c_2)x + (a_0 + a_2c_1c_2)z\big]\\
&\quad + \frac{2xz}{c_p^2 - c_s^2}\big(b_0 - b_1c_s^2 - b_2c_p^2\big),\\
u^{(3)} &= b_0t^2 + b_1x^2 + b_2z^2 + \frac{2t}{c_1+c_2}\big[(b_0 + b_1c_1c_2)x + (b_0 + b_2c_1c_2)z\big]\\
&\quad + \frac{2xz}{c_p^2 - c_s^2}\big(a_0 - a_1c_p^2 - a_2c_s^2\big).
\end{aligned}$$

This provides an additional growing mode that is not present in the scalar case. For the specific choice $a_1 = a_2 = b_1 = b_2 = 0$, $a_0 = 1$, $b_0 = 0$, we find

$$u^{(1)} = t\left(t + \frac{2(x+z)}{c_1+c_2}\right).$$

This may be interpreted as a wave that travels out of the domain, but has an amplitude that grows linearly in time. The t^2 term will eventually dominate the behaviour. This is clearly an unwanted mode. To suppress this mode, we use a first-order implicit scheme (23) which is dissipative by itself, in contrast to the second-order implicit scheme (see appendix A). In addition, we increase the damping parameters. The resulting boundary scheme is the same as (21), but with

$$R_j = 1 - \frac{z^{-1} + \nu_j T}{1 + \nu_j}.$$

The corners of the domain are a known source of trouble [2, 18, 27]. For the wave and acoustic equation, we did not encounter any problems. In the elastic case, the combination of the damping in the first-order implicit scheme and the lower accuracy due to larger values of ε_i appears to counteract any corner instabilities that may occur.

Another complication in the elastic case is the fact that the one-dimensional extrapolation from interior data does not provide data in the corner regions. Here we again follow Higdon's approach [18]. First the extrapolation is carried out in one coordinate direction, right up to the corner, and thus ignoring the fact that some of the interior data actually originate from another boundary strip. These data are therefore invalid. Next, the update is done for the second coordinate direction, followed by the third (in three space dimensions). The last update always provides correct data. The order in which the various boundary strips are visited is altered for each subsequent time step.

For the elastic system of equations, I have only implemented the extrapolation on each field separately. In principle, a one-dimensional system could be used, leading to

$$\left[\prod_{i=1}^{M} \left(\partial_t - A_i^{(x)} \partial_x \right) \right] \boldsymbol{u} = 0, \tag{22}$$

where $A_i^{(x)}$ is a coefficient matrix that needs to be tuned to minimise the reflection off the absorbing boundary. This scheme remains to be explored.

Note that the material properties have been assumed to be constant in the boundary strip. Also, they must be constant in the interior in a strip of width M to avoid instabilities. If unwanted diffraction patterns are to be avoided, this implies that the earth model must be constant in the direction perpendicular to the boundary across some width near the boundary.

The boundary conditions should be initialised with zero data. This implies that the solution should be zero near the boundary at the start of the computation.

Suggestions for the choice of the c_i and ε_i are given next. For the simple wave equation and the acoustic equation, we choose $c_1 = c$, $c_2 = 2\,c$, $c_3 = 1.25\,c$, and $\varepsilon_1 = 0$, $\varepsilon_2 = 0.05$. In the isotropic elastic case, we use $c_1 = c_s$, $c_2 = c_p$, and $c_3 = 2\,c_p$. Here c_p and c_s are the P- and S-wave velocities. A first-order implicit scheme is used with $\varepsilon_1 = 10^{-3}$ and $\varepsilon_2 = 0.1$. In the anisotropic case, we compute the eigenvalues of a 3×3 submatrix of the elasticity tensor, divided by the density. The

submatrix is obtained by selecting only those elements that are related to x-derivatives, i.e., $C^{(k,1,m,1)}/\rho$. The square-root of the smallest eigenvalue is assigned to c_1, of the intermediate to c_2, whereas the square-root of the largest is multiplied by 1.5 and assigned to c_3.

4. Examples

We present a set of numerical results to illustrate the performance of Higdon's boundary conditions for some simple cases. The interior scheme is of order 8 and the time integration of order 2, except for the anisotropic case where the interior scheme is of order 6.

A test problem is sketched in figure 1 and consists of a homogeneous medium with a velocity of 2.5 km/s. In the elastic case, we use $c_p = 2.5$ km/s, $c_s = 1.25$ km/s, and constant density. The domain size in the two-dimensional case is $400 \times 400\,\mathrm{m}^2$. At the top ($z = 0$ m), a free-surface boundary condition is used; at the bottom ($z = 400$ m), the absorbing boundary condition is applied. The other boundary conditions are based on symmetry: the pressure (wave and acoustic equation) or displacement field (elastic equation) is mirrored with the same sign, except for the displacement component in the direction perpendicular to the boundary, which is mirrored with opposite sign. At the boundary where the source is located, the symmetry boundary acts as a true line of symmetry; at the opposite boundary it acts as a hard reflector. In this way, we can simulate a wide range of angles of incidence at the absorbing boundary within a small computational domain.

An explosive source is placed at $x_s = 0$ m and $z_s = 150$ m. Traces of the pressure (for the wave equation) or the vertical displacement (in the elastic case) have been recorded at a depth of 400 m for 0.5 s. For the three-dimensional examples, the source is placed on the intersection of a symmetry boundary in x and in y. The opposite x-boundary is symmetric and reflecting as in the two-dimensional example. The opposite y-boundary is placed sufficiently far away, so that reflected waves cannot reach the receiver line at $y = 0$ m, $z = 400$ m.

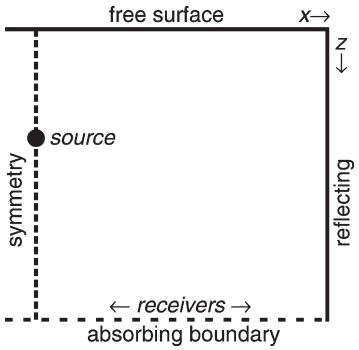

Figure 1. Definition of the two-dimensional test problem.

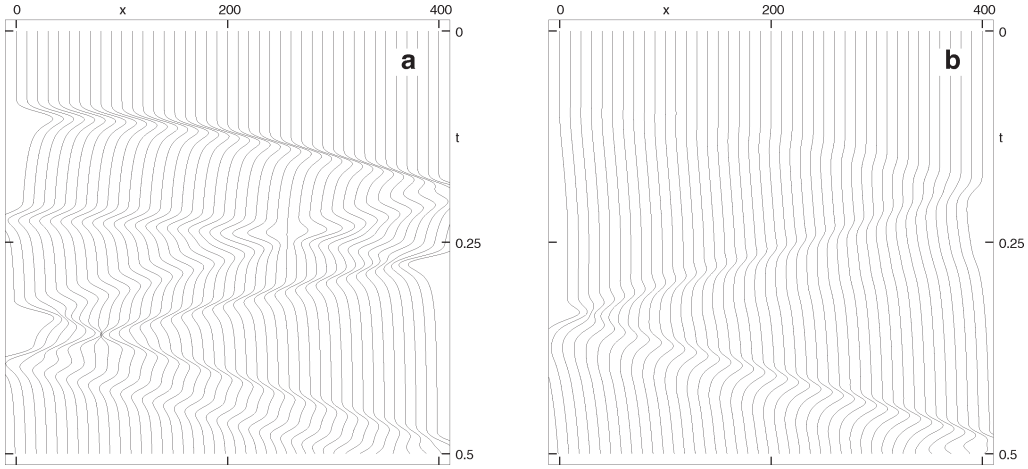

Figure 2. Receiver traces of the pressure for the 2D test problem are shown in the left figure. On the right, the energy reflected by the absorbing boundary is shown. The result has been obtained by subtracting traces for perfect absorbing boundary conditions from those in the left figure. The amplitude scale of the right figure has been boosted by a factor 10 as compared to the left figure.

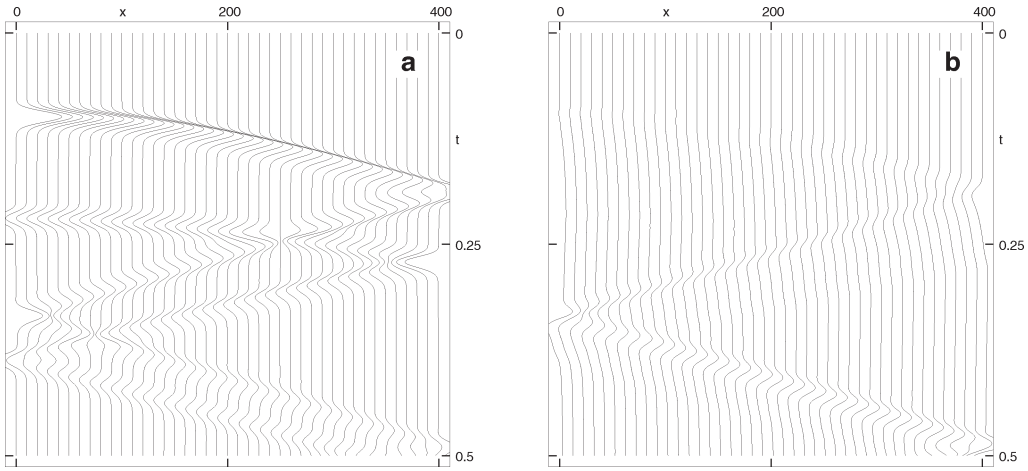

Figure 3. Pressure traces for the 3D test problem. The reflections off the absorbing boundary are plotted in the right figure. The amplitude scale has been boosted by a factor 10 as compared to the left figure.

The results have been compared to solutions obtained for a larger model that extends to greater depth so that reflections off the bottom cannot reach the receivers.

Figure 2a shows traces for the simple wave equation. Third-order boundary conditions are used, with second-order differencing in space and time for each factor in (21). Figure 2b shows the reflected energy. This picture has been obtained by subtracting the traces for the larger model from those in figure 2a. Note that figures 2a and 2b have different scales. The deterioration of the absorbing boundary condition for larger angles of incidence (occurring at later time) is obvious. Also note the long-wave reflection at small angles of incidence that can be clearly seen at $x = 0$, starting

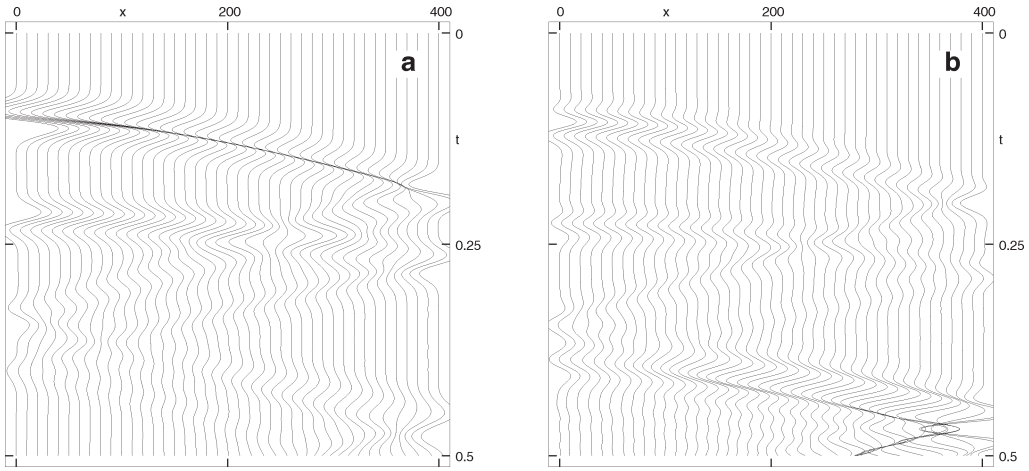

Figure 4. Receiver traces of the z-displacement for a 2D elastic model. The reflections off the absorbing boundary are plotted in the right figure. The amplitude scale has been boosted by a factor 5 as compared to the left figure.

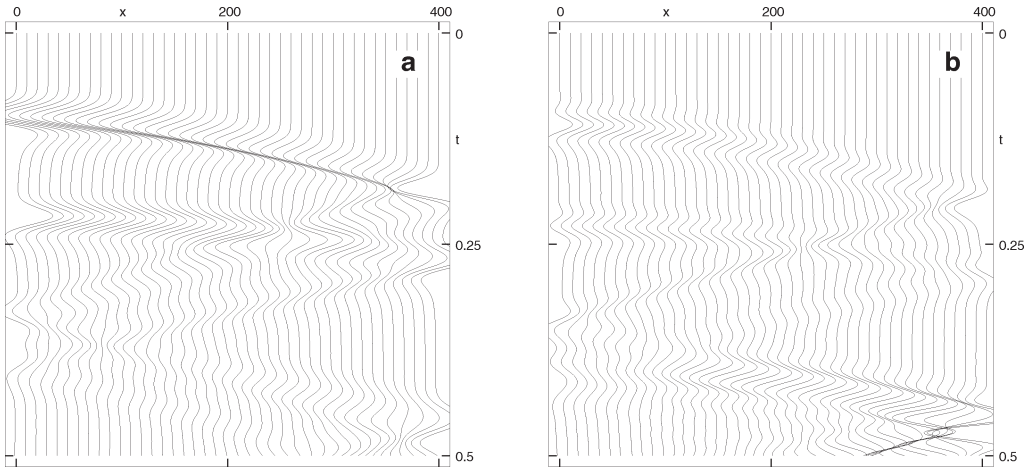

Figure 5. Traces for a 3D elastic model. Shown is the z-displacement. The reflections off the absorbing boundary are plotted in the right figure. The amplitude scale has been boosted by a factor 5 as compared to the left figure.

at the first arrival. Similar results for a three-dimensional computation are shown in figures 3a and 3b.

We have used a different interior numerical scheme for the acoustic case. The results are almost indistinguishable from those for the wave equation shown in figures 2 and 3, and are therefore omitted.

Traces of the z-displacement for the two-component elastic case (P-SV) in two space dimensions are shown in figure 4. Results for the three-component three-dimensional case are displayed in figure 5. Note that the reflections off the absorbing boundary are markedly stronger than in the scalar case.

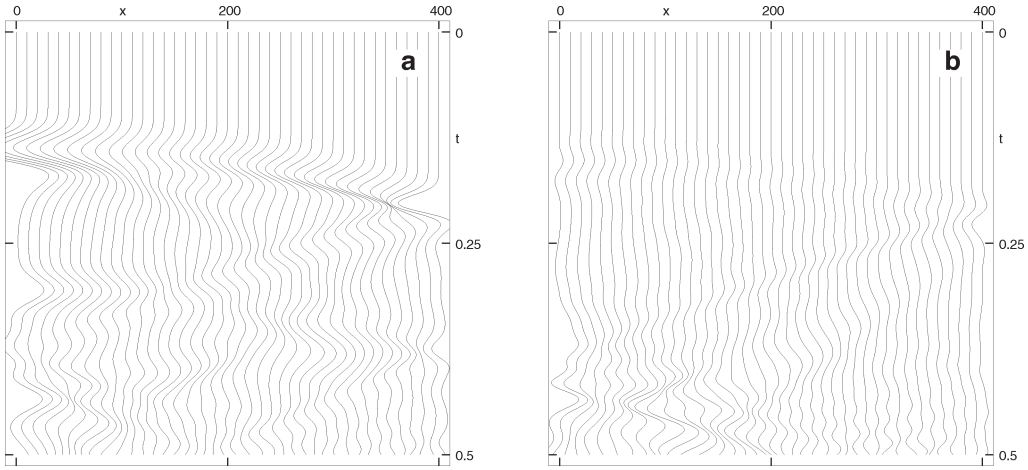

Figure 6. Traces for a 2D anisotropic model. Shown is the z-displacement. The reflections off the absorbing boundary are plotted in the right figure. The amplitude scale has been boosted by a factor 2 as compared to the left figure.

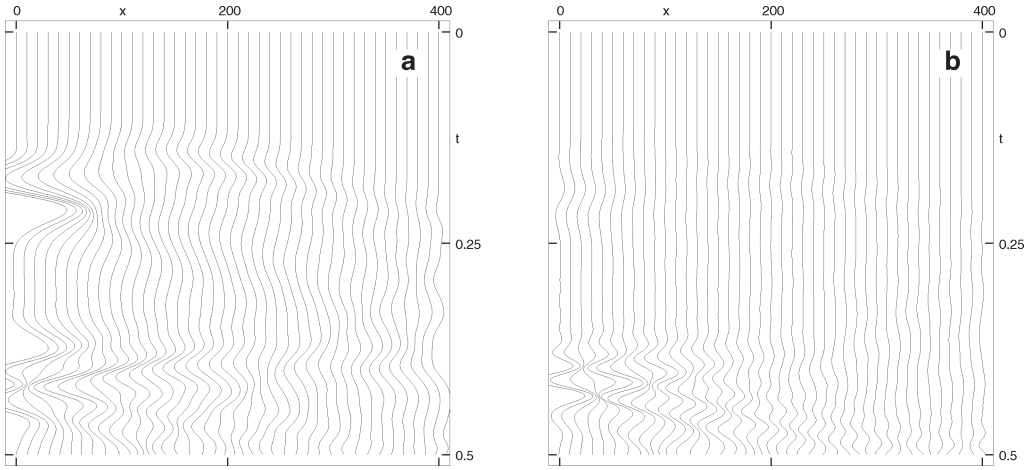

Figure 7. Traces for a 3D anisotropic model. Shown is the z-displacement. The reflections off the absorbing boundary are plotted in the right figure. The amplitude scale has been boosted by a factor 2 as compared to the left figure.

As an example for the anisotropic elastic case, we have used the same anisotropic triclinic medium as in [19], rescaled to a maximum velocity of 2.5 km/s. Traces of the z-displacement are shown in figures 6 and 7. Note that the reflections off the absorbing boundary are stronger than in the isotropic case.

The results from figures 2–7 are summarised in table 1, where the ratio of the maximum amplitude in the traces and in the reflected waves is given. This ratio provides a crude indication of the quality of the absorbing boundary condition, mainly determined by waves impinging at large angles of incidence. In practice, these waves

Table 1
Ratio of maximum amplitude in the reflected and original traces.

Equation	2D	3D
wave	0.085	0.053
isotropic elastic	0.215	0.234
anisotropic elastic	0.217	0.238

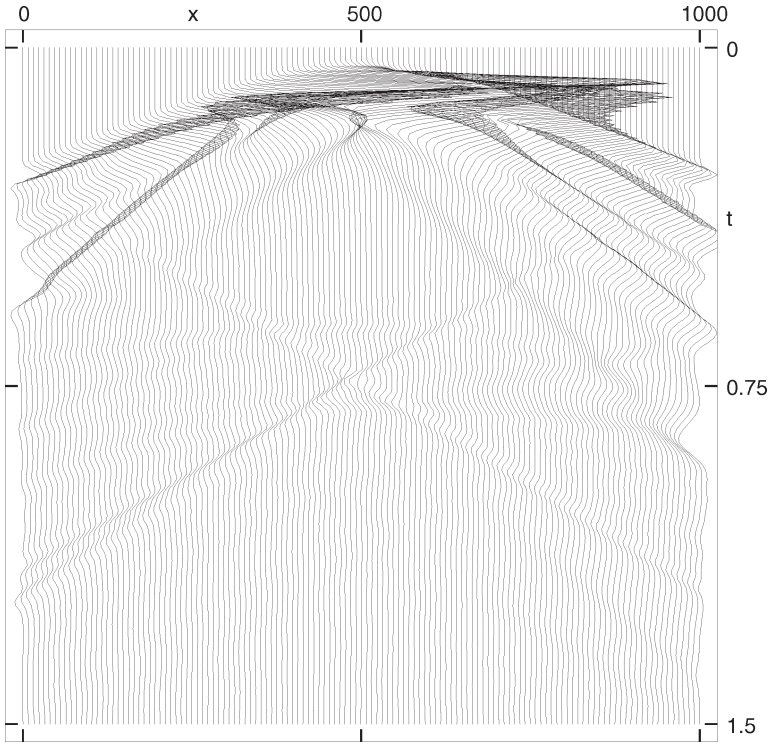

Figure 8. Traces of the z-displacement for a 2D anisotropic elastic model.

are of less importance as they are confined to a region near the boundary. In this sense, the results of table 1 are to be considered as worst case.

Another example for the anisotropic case is shown in figure 8. The traces have been obtained for the same triclinic medium as above, but with absorbing boundaries on all four sides. The domain size is $1000 \times 1000\,\mathrm{m}^2$. An explosive source has been fired in the centre of the domain. Traces are read off at a depth of 375 m. The reflection of the primary wave is clearly visible. At times later than 0.75 s, a disturbance can be seen at the right-hand side of the figure which is related to reflection of the shear wave.

As a last example, we show traces for a part of the two-dimensional Marmousi model. The velocity model is shown in figure 9. Traces are displayed in figure 10. There are no visible reflections off the artificial boundary.

The numerical experiments show that Higdon's boundary conditions of third order perform well for high-order discretisations of the wave and acoustic equation.

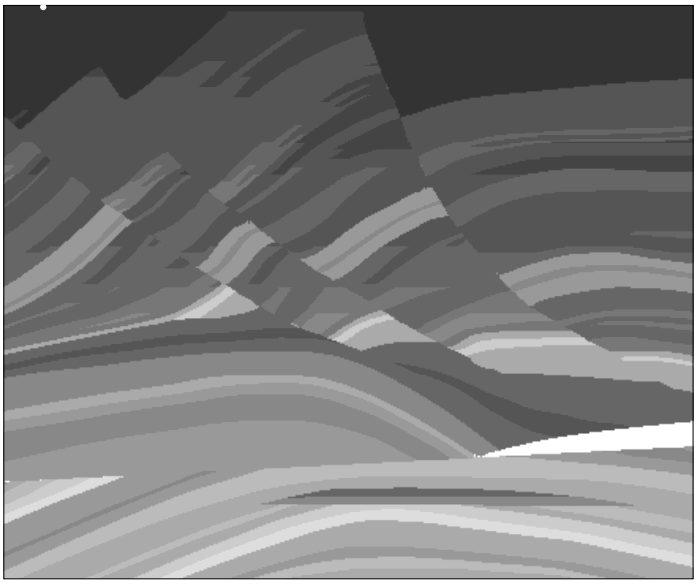

Figure 9. Part of the Marmousi model. The source is marked by a dot near the left upper corner.

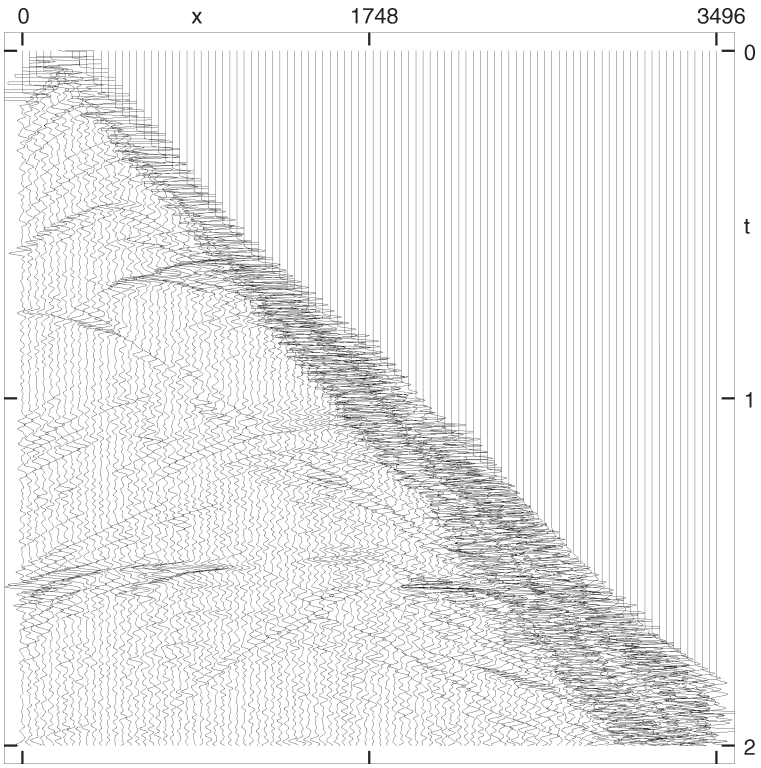

Figure 10. Pressure traces for part of the Marmousi model. The larger amplitudes have been clipped.

Reasonable results are obtained for the isotropic elastic case and almost reasonable results in the strongly anisotropic example. The system approach (22) might add some improvement here, but this remains to be investigated.

5. Conclusions

We have reviewed various ideas that may guide the construction of absorbing boundary conditions for wave propagation problems. A fundamental problem in the construction of accurate absorbing boundary conditions has been encountered: highly accurate conditions allow for growing modes such as xt that are solutions of the second-order wave equation but are unwanted in practical computations. These modes can be avoided by using conditions of lower accuracy, but this will increase the amount of reflected energy. We have found an additional growing low-frequency mode in the elastic case, which will occur if higher-order local boundary conditions are used.

As a compromise between accuracy and the suppression of growing low-frequency modes, Higdon's boundary conditions have been chosen. These conditions are relatively easy to implement. Numerical experiments show acceptable results for the simple and acoustic wave equation, and close to reasonable results for the isotropic and anisotropic elastic case. The slowly growing long-wave modes can be suppressed by damping. There is a trade-off between the increase in damping needed to suppress the growing modes and the decrease in damping needed to reduce the amount of reflected energy. Practical values for the amount of damping have been given. For very long integration times, however, the low-frequency modes may still show up.

Acknowledgements

The author is indebted to J. N. Buur for his programming assistance.

Appendix A: One-dimensional boundary operators

Here we present a few simple one-sided approximations to the equation $u_t = cu_x$, $c > 0$, for a "left" boundary. Recall that the grid spacing is Δx and $x_j = j\Delta x$. The time step is Δt and time is $t^n = n\Delta t$. The discrete solution at (t^n, x_j) is denoted by u_j^n. The shift operator in space is T and in time is z, i.e., $T^m u_j^n = u_{j+m}^n$ and $z^m u_j^n = u_j^{n+m}$. Abbreviate $\nu = c\Delta t/\Delta x$. The first point at the left boundary sits at $j = 0$. In the Fourier domain, $\widehat{T} = \exp(\mathrm{i}\xi)$, with $|\xi| \leq \pi$. The exact operator has the Fourier symbol $\widehat{z}_e = \exp(\mathrm{i}\nu\xi)$.

A first-order explicit scheme is given by

$$\left(1 - z^{-1}\right) = z^{-1}\nu(T - 1),$$

and has an amplification factor for the time stepping scheme

$$|\widehat{z}|^2 = 1 - 4\nu(1-\nu)\sin^2(\xi/2),$$

which implies stability for $\nu \leqslant 1$. A first-order implicit scheme reads

$$\left(1 - z^{-1}\right) = \nu(T-1), \tag{23}$$

and has

$$|\widehat{z}|^2 = \frac{1}{1 + 4\nu(1-\nu)\sin^2(\xi/2)},$$

implying unconditional stability. A second-order implicit one-sided approximation is

$$\tfrac{1}{2}(1+T)\left(1 - z^{-1}\right) = \nu\tfrac{1}{2}\left(1 + z^{-1}\right)(T-1), \tag{24}$$

and has $|\widehat{z}|^2 = 1$. Note that this scheme conserves energy, whereas the first-order schemes are dissipative.

Appendix B: Discretisations

For the temporal discretisation, a cheaper variant of the scheme presented by Dablain [6] is used. Let u be the scalar or vector-valued solution. An additional subscript refers to position and a superscript to a time value $t^n = n\Delta t$. Dablain's scheme reads

$$u_i^{n+1} = 2u_i^n - u_i^{n-1} + \sum_{m=1}^{N_x/2} \frac{2}{(2m)!}(\Delta t)^{2m} \frac{\partial^{2m} u_i^n}{\partial t^{2m}}.$$

Given a spatial operator L for a wave equation $u_{tt} = Lu$, we have

$$\frac{\partial^{2m} u}{\partial t^{2m}} = L^m u,$$

i.e., the spatial operator is applied repeatedly. Let $L_{\{n\}}$ be a discretisation of spatial order n. Then a scheme of order N_t in time and N_x in space, N_t and N_x even, is obtained by approximating

$$\frac{\partial^{2m} u}{\partial t^{2m}} \simeq \left[\prod_{k=1}^{m} L_{\{N(k)\}}\right] u, \quad N(k) = \max\left(2, N_x - 2(k-1)\right),$$

that is, the order of the spatial scheme is reduced by 2 for each iteration following the first. This may be less expensive, depending on computer hardware properties, than the common approach in which $N(m) = N_x$. Here it should also be taken into

account that the schemes have different stability properties. Such issues, however, are beyond the scope of this paper.

The spatial discretisation for the simple wave equation (14) involves a direct evaluation of the second derivative in each coordinate. Let T_x be the shift operator in the x-direction: $T_x^m u_{i,j,k} = u_{i+m,j,k}$. Here $u_{i,j,k}$ represents the value of u at position (x_i, y_j, z_k) on a regular grid, i.e., $x_i = i\Delta x$, $y_j = j\Delta y$, $z_k = k\Delta z$ where Δx, Δy, and Δz are constant grid spacings. Define $M = N_x/2$. The second derivative operator in the x-direction is discretised by

$$D_{xx} = -\frac{1}{\Delta x^2}\left[w_0 + \sum_{m=1}^{M} w_m \big(T_x^m + T_x^{-m}\big) \right],$$

where

$$w_0 = \sum_{k=1}^{M} \frac{2}{k^2}, \qquad w_m = (-1)^m \sum_{k=m}^{M} \frac{2}{k^2} \frac{(k!)^2}{(k-m)!(k+m)!}, \quad 1 \leqslant m \leqslant M.$$

The expressions for the y- and z-directions are similar.

Staggered finite differences are used for the acoustic equation (15). The first derivative in the x-direction is discretised by

$$D_x = \frac{1}{\Delta x}\left[\sum_{m=1}^{M} w'_m \big(T_x^{m-1/2} - T_x^{1/2-m}\big) \right],$$

where

$$w'_m = \frac{(-1)^{(m+1)}}{(m-1/2)^2} \frac{m+M}{2^{4M}} \binom{2M}{M+m} \binom{2M}{M}. \tag{25}$$

This operator places the result half-way between two grid points. Multiplying the result by ρ^{-1} and applying the operator again, produces a result at the original unstaggered location of $u_{i,j,k}$.

A staggered finite-difference scheme [19, 25, 35, 36] is used for the spatial discretisation of the 3-component elastic wave equation. The displacements are represented at staggered location: given a uniform grid with points $x_{i,j,k}$ as above, the x-displacements $u^{(1)}$ are represented at positions $x_{i,j,k} + \frac{1}{2}\Delta x$, the y-displacements $u^{(2)}$ at $x_{i,j,k} + \frac{1}{2}\Delta y$, and the z-displacements $u^{(3)}$ at $x_{i,j,k} + \frac{1}{2}\Delta z$. First derivatives are computed as in [19], but using the weights (25). In the anisotropic case, interpolation is required from staggered to unstaggered location and vice versa. We use an interpolation operator of the same order as the first-derivative operator. In the x-direction, the interpolation operator is given by

$$I_x = \sum_{m=1}^{M} w_m \big(T_x^{m-1/2} + T_x^{1/2-m}\big),$$

where $w_m = (m - 1/2)w'_m$.

References

[1] A. Bamberger, B. Chalindar, P. Joly, J. E. Roberts and J. L. Teron, Absorbing boundary conditions for Rayleigh waves, SIAM J. Sci. Statist. Comput. 9 (1988) 1016–1049.

[2] A. Bamberger, P. Joly and J. E. Roberts, Second-order absorbing boundary conditions for the wave equation: a solution for the corner problem, SIAM J. Numer. Anal. 27 (1990) 323–352.

[3] J. Broeze and E. F. G. van Daalen, Radiation boundary conditions for the two-dimensional wave equation from a variational principle, Math. Comp. 58 (1992) 73–82.

[4] C. Cerjan, D. Kosloff, R. Kosloff and M. Reshef, A nonreflecting boundary condition for discrete acoustic and elastic wave equations, Geophysics 50 (1985) 705–708.

[5] R. Clayton and B. Engquist, Absorbing boundary conditions for acoustic and elastic wave equations, Bull. Seismol. Soc. Amer. 67 (1977) 1529–1540.

[6] M. A. Dablain, The application of higher-order differencing to the scalar wave equation, Geophysics 51 (1986) 54–66.

[7] B. Engquist and A. Majda, Absorbing boundary conditions for the numerical simulation of waves, Math. Comp. 31 (1977) 629–651.

[8] B. Engquist and A. Majda, Radiation boundary conditions for acoustic and elastic wave calculations, Comm. Pure Appl. Math. 32 (1979) 313–357.

[9] D. Givoli, Non-reflecting boundary conditions, J. Comput. Phys. 94 (1991) 1–29.

[10] M. Goldberg and E. Tadmor, Scheme-independent stability criteria for difference approximations of hyperbolic initial-boundary value problems II, Math. Comp. 36 (1981) 603–626.

[11] B. Gustafsson, H.-O. Kreiss and A. Sundström, Stability theory of difference approximations for mixed initial boundary value problems II, Math. Comp. 26 (1972) 649–686.

[12] B. Gustafsson, The convergence rate for difference approximations to mixed initial boundary value problems, Math. Comp. 29 (1975) 396–406.

[13] B. Gustafsson, The convergence rate for difference approximations to general mixed initial boundary value problems, SIAM J. Numer. Anal. 18 (1981) 179–190.

[14] B. Gustafsson, Inhomogeneous conditions at open boundaries for wave propagation problems, Appl. Numer. Math. 4 (1988) 3–19.

[15] B. Gustafsson, H.-O. Kreiss and J. Oliger, *Time Dependent Problems and Difference Methods* (Wiley, New York, 1995).

[16] R. L. Higdon, Absorbing boundary conditions for difference approximations to the multi-dimensional wave equation, Math. Comp. 47 (1986) 437–459.

[17] R. L. Higdon, Numerical absorbing boundary conditions for the wave equation, Math. Comp. 49 (1987) 65–90.

[18] R. L. Higdon, Radiation boundary conditions for elastic wave propagation, SIAM J. Numer. Anal. 27 (1990) 831–870.

[19] H. Igel, P. Mora and B. Riollet, Anisotropic wave propagation through finite-difference grids, Geophysics 60 (1995) 1203–1216.

[20] M. Israeli and S. A. Orszag, Approximation of radiation boundary conditions, J. Comput. Phys. 41 (1981) 115–135.

[21] H.-O. Kreiss, Initial boundary value problems for hyperbolic systems, Comm. Pure Appl. Math. 23 (1970) 277–298.

[22] R. Kosloff and D. Kosloff, Absorbing boundaries for wave propagation problems, J. Comput. Phys. 63 (1986) 363–376.

[23] Z. P. Liao, H. L. Wong, Y. Baipo and Y. Yifan, A transmitting boundary for transient wave analyses, Scientia Sinica 27 (1984) 1063–1076.

[24] E. L. Lindman, “Free-space” boundary conditions for the time dependent wave equation, J. Comput. Phys. 18 (1975) 66–78.

[25] R. Madariaga, Dynamics of an expanding circular fault, Bull. Seismol. Soc. Amer. 66 (1976) 639–666.

[26] D. Michelson, Stability theory of difference approximations for multidimensional initial-boundary value problems, Math. Comp. 40 (1983) 1–45.
[27] S. Osher, Hyperbolic equations in regions with characteristic boundaries or with corners, in: *Numerical Solution of Partial Differential Equations III*, ed. B. Hubbard (Academic Press, New York, 1976) pp. 413–441.
[28] R. J. Randall, Absorbing boundary conditions for the elastic wave equation, Geophysics 53 (1988) 611–624.
[29] W. D. Smith, A nonreflecting plane boundary for wave propagation problems, J. Comput. Phys. 15 (1974) 492–503.
[30] J. Sochacki, R. Kubichek, J. George, W. R. Fletcher and S. Smithson, Absorbing boundary conditions and surface waves, Geophysics 52 (1987) 60–71.
[31] K. W. Thomson, Time-dependent boundary conditions for hyperbolic systems II, J. Comput. Phys. 89 (1990) 439–461.
[32] L. N. Trefethen, Instability of difference models for hyperbolic initial boundary value problems, Comm. Pure Appl. Math. 37 (1984) 329–367.
[33] L. N. Trefethen, Stability of finite-difference models containing two boundaries or interfaces, Math. Comp. 45 (1985) 279–300.
[34] L. N. Trefethen and L. Halpern, Well-posedness of one-way wave equations and absorbing boundary conditions, Math. Comp. 47 (1986) 421–435.
[35] J. Virieux, SH-wave propagation in heterogeneous media: Velocity-stress finite difference method, Geophysics 49 (1984) 1933–1942.
[36] J. Virieux, P-SV wave propagation in heterogeneous media: Velocity-stress finite difference method, Geophysics 51 (1986) 889–901.